1D4-4

Measurement Based Parametric Channel Modeling Considering Diffuse Scattering and Specular Components

Markus Landmann [1], Martin Kaeske [1], Reiner Thoma [1], Jun-ichi Takada [2], Ichirou Ida [3]
[1] Institute of Information Technology, Ilmenau University of Technology
Ilmenau, Germany, markus.landmann@tu-ilmenau.de
[2] Graduate School of Engineering, Tokyo Institute of Technology
Tokyo, Japan, takada@ide.titech.ac.jp
[3] Fujitsu Limited
Tokyo, Japan, ida.ichirou@jp.fujitsu.com

1. Introduction

Efficient design of MIMO transmission systems requires a thorough understanding of the multi-dimensional structure of the mobile radio channel. Widely accepted for a measurement based channel characterisation are parameter estimation algorithm like ESPRIT [1] and SAGE [2]. The idea is to deduce a parametric model of the MIMO channel. Hereby the channel is modelled by a number of individual specular propagation paths that are described by the parameters direction of arrival (DoA),direction of departure (DoD), time delay of arrival (TDoA) and the complex polarimetric path weights, which are independent from the antennas used during the measurement. A first approach to use these estimated parameters of the specular components (SC) for measurement based parametric channel modelling (MBPCM) was proposed in [3]. It offers the possibility to emulate the MIMO transfer properties of arbitrary antenna arrays by reconstructing the hypothetical antenna response from the estimated channel parameters. However, it was observed that with the specular paths only 20% to 50% of the received signal power can be described. Therefore, the RIMAX algorithm [4] decribes the channel by a superposition of specular components, and dense multipath components (DMC) that mainly result from distributed diffuse scattering. Nevertheless, so far only the contribution of the SCs are used for the MBPCM. Consequently, it was observed [5], [6] that the MIMO capacity calculated from the reconstructed channels using only the SCs are lower compared to the ones calculated from the measurements. In this contribution the MBPCM approach is applied comprising both components the SCs and the DMCs, where measurement data of a macro cell scenario and the corresponding RIMAX parameter estimation results are used. The MIMO capacities calculated from the measured channel, reconstructed channel based on the SCs, reconstructed channel based on SCs and DMCs, and the reconstructed channel superposing the SCs, DMCs and an artificial measurement noise are compared.

2. Channel measurement and characterisation

The full polarimetric double directional channel measurements are performed in a macro-cell environment in Tokyo[1]. A RUSK channel sounder [7] at a center frequency of 4.5 GHz and a signal bandwidth of 120 MHz is used. The transmit antenna array (Tx), a 2×4 polarimetric uniform rectangular patch array (PURPA) is placed over roof top at a 10 floor high building (35 m). The receive antenna array (Rx), a 2×24 stacked polarimetric uniform circular patch array (SPUCPA) is placed at a cart around 1.6 m above the street, where the buildings in the surrounding residential area are between two and three flours high. The measurement conditions vary between pure line of sight (LoS), mixed non LoS (NLoS) and obstructed LoS (OLoS) and pure NLoS . In total ca. 1600 snapshots were recorded along the 490 m long measurement route, where each snapshot consists of 1536 complex impulse responses with a maximum excess delay of 3.2 μs. To deduce the parameters of the SCs and the DMCs from the measured data $\mathbf{x}$, the estimation algorithm RIMAX [4] is used. With the stationary measurement noise $\mathbf{n}$ and the dense multipath and specular components $\mathbf{d}$ and $\mathbf{s}$ respectively, the total observed signal vector $\mathbf{x}$ is modelled as follows:

$$\mathbf{x}^{[M_{\mathrm{Rx}} \cdot M_{\mathrm{Tx}} \cdot M_{\mathrm{f}} \times 1]} = \mathbf{n} + \mathbf{d}(\boldsymbol{\theta}_{\mathrm{DMC}}) + \sum_{k=1}^{K} \mathbf{s}(\boldsymbol{\theta}_k) \tag{1}$$

[1]This measurement is supported by the National Institute of Information and Communications Technology of Japan.

ISBN: 978-4-88552-223-9 C3055©IEICE

where the superscript [.] denotes the size of the vector, M_{Rx} and M_{Tx} are the number of Rx and Tx antennas respectively and M_{f} is the number of frequency bins. The vector $\boldsymbol{\theta}_k$ includes the parameters of the k^{th} **SC** characterised by its DoD ($\varphi_{\mathrm{T}k}$, $\vartheta_{\mathrm{T}k}$ (azimuth and elevation)), TDoA τ_k, DoA ($\varphi_{\mathrm{R}k}$, $\vartheta_{\mathrm{R}k}$), and the four complex polarimetric path weights $\gamma_{\mathrm{hh},k}$, $\gamma_{\mathrm{hv},k}$, $\gamma_{\mathrm{vv},k}$, $\gamma_{\mathrm{vh},k}$, where the first subscript indicates the polarisation at the base station and the second at mobile station. The second part of the data model, the DMC, are considered as the remaining complex impulse responses after removing the contribution of the reliable estimated SCs and measurement noise. Resulting from many observations of measured channel responses, an exponential decaying data model is defined to represent the DMC in the delay (correlation) domain $\psi_{xy}(\tau)$ with its corresponding frequency response $\Psi_{xy}(f)$:

$$\begin{aligned}
\psi_{xy}(\tau) &= E\{|h_{xy}(\tau)|^2\} = \left\{ \begin{array}{cc} 0 & \tau < \tau_{\mathrm{n,xy}} \\ \alpha_{1,xy} \cdot \frac{1}{2} & \tau = \tau_{\mathrm{n,xy}} \\ \alpha_{1,xy} \cdot e^{-\beta_{\mathrm{d,xy}}(\tau-\tau_{\mathrm{n,xy}})} & \tau > \tau_{\mathrm{n,xy}} \end{array} \right\} \\
\mathcal{F} & \;\updownarrow \\
\Psi_{xy}(f) &= \frac{\alpha_{1,xy}}{\beta_{\mathrm{d,xy}} + j2\pi f} \cdot e^{-j2\pi f \tau_{\mathrm{n,xy}}}
\end{aligned} \tag{2}$$

where $\beta_{\mathrm{d,xy}}$ is the normalised coherence bandwidth, $\tau_{\mathrm{n,xy}}$ is the base delay and $\alpha_{1,xy}$ is the maximum DMC power, h_{xy} is a channel impulse response with transmit and receive polarisation x and y respectively ((horizontal (h) or vertical (v))). As proposed in [8] the distribution of the DMC is estimated independently for all four polarisation combinations from the corresponding mean power delay profiles. The parameter vector of the DMCs is defined with $\boldsymbol{\theta}_{\mathrm{DMC}} = [\boldsymbol{\theta}_{\mathrm{DMChh}},\ \boldsymbol{\theta}_{\mathrm{DMChv}},\ \boldsymbol{\theta}_{\mathrm{DMCvh}},\ \boldsymbol{\theta}_{\mathrm{DMCvv}}]$. Each vector $\boldsymbol{\theta}_{\mathrm{DMCxy}}$ is composed of the parameters $[\alpha_{1,xy}, \beta_{\mathrm{d},xy}, \tau_{\mathrm{n},xy}]$. Furthermore, the mean measurement noise power at one frequency bin is estimated and corresponds to α_0 .

3. Channel reconstruction and capacity calculation

For the capacity analysis four cases of channel matrices are considered, the measured channel matrices (**Meas**), the reconstructed based on the specular components **s** (**SC**) only, the reconstructed SCs superposed with the reconstructed DMCs **d** (**SC+DMC**), and the reconstructed SCs superposed with the reconstructed DMCs and artificial measurement noise with the same mean noise power α_0 as estimated from the measurement (**SC+DMC+Noise**). For the channel reconstruction the data model as described in eqn. (1) is used. The contribution of the k^{th} SC is reconstructed using:

$$\begin{aligned}
\mathbf{s}(\boldsymbol{\theta}_k) = \mathbf{b}_{\mathrm{R_h},k} \otimes \mathbf{b}_{\mathrm{T_h},k} \otimes \mathbf{b}_{f,k} \cdot \gamma_{\mathrm{hh,k}} + \mathbf{b}_{\mathrm{R_v},k} \otimes \mathbf{b}_{\mathrm{T_h},k} \otimes \mathbf{b}_{f,k} \cdot \gamma_{\mathrm{hv,k}} + \\
\mathbf{b}_{\mathrm{R_h},k} \otimes \mathbf{b}_{\mathrm{T_v},k} \otimes \mathbf{b}_{f,k} \cdot \gamma_{\mathrm{vh,k}} + \mathbf{b}_{R_v,k} \otimes \mathbf{b}_{T_v,k} \otimes \mathbf{b}_{f,k} \cdot \gamma_{\mathrm{vv,k}}
\end{aligned} \tag{3}$$

where $\mathbf{b}_{\mathrm{R_{x,k}}}$, $\mathbf{b}_{\mathrm{T_{y,k}}}$ define the k^{th} polarimetric array response at the receive and transmit side respectively, $\mathbf{b}_{f,k}$ denotes the frequency response, and $\otimes$ denotes the Kronecker product. The DMC component **d** is modelled as a stochastic process with the covariance matrix $\mathbf{R}_{xy}$, which is calculated by using the sampled version of the frequency response $\Psi_{xy}(f)$ as defined in equation (2).

$$\mathbf{R}_{\mathrm{xy}} = \mathrm{toep}^2(\kappa(\boldsymbol{\theta}_{\mathrm{DMCxy}})\kappa(\boldsymbol{\theta}_{\mathrm{DMCxy}})^H) \quad , \text{ with } \quad \kappa(\boldsymbol{\theta}_{\mathrm{DMCxy}}) = \left[\Psi_{xy}(0)\, \Psi_{xy}(\Delta f) \cdots \Psi_{xy}((M_f - 1)\cdot \Delta f)\right]^T \in C^{M_f \times 1} \tag{4}$$

For each channel an adequate random vector is created by using an i.i.d. circular Gaussian process $\mathbf{z}_i$:

$$\mathbf{z}_i \in C^{M_f \times 1} \sim \mathcal{N}_c(\mathbf{0}, \mathbf{I}),\ i = 1 \ldots M_{Tx} \cdot M_{Rx} \tag{5}$$

and applying the transformation matrix **L** w.r.t. the xy polarisation combination of the i^{th} channel:

$$\mathbf{d}_i(\boldsymbol{\theta}_{DMCxy}) = \mathbf{L}(\boldsymbol{\theta}_{DMCxy}) \cdot \mathbf{z}_i \Rightarrow \mathbf{d}(\theta_{DMC}) = \left[\mathbf{d}_1^T \ \ldots \ \mathbf{d}_{M_{Rx}\cdot M_{Tx}}^T\right]^T \tag{6}$$

where the matrix $\mathbf{L}_{xy}$ is obtained by the Cholesky decompostion of $\mathbf{R}_{xy} = \mathbf{L}_{xy} \cdot \mathbf{L}_{xy}^H$. In case of the noise affected reconstruction each element of **n** is defined as:

$$n \sim N(0; \frac{\sigma 2}{2}) + \mathrm{j} \cdot N(0; \frac{\sigma 2}{2}), \tag{7}$$

where σ is set to the square root of the mean estimated noise power α_0.

[2] toep(a, b) returns a toeplitz matrix with a as its first column and b as its first row

The instantenous capacity of a frequency selective channel is defined as the mean capacity over all frequency bins:

$$C \;=\; \frac{1}{M_f}\sum_{m_f=0}^{M_f-1} log_2\left(1+\frac{\rho}{M_{Tx}}\widehat{\mathbf{H}}(\Delta f\cdot m_f)\cdot\widehat{\mathbf{H}}^H(\Delta f\cdot m_f)\right) \tag{8}$$

where ρ is the mean signal to noise ratio (SNR). Note that this SNR will be called application SNR and is **not** related to the SNR of the measurement. In order to compare the capacities of the channels $\mathbf{H}_{\text{Meas}}$, $\mathbf{H}_{\text{SC}}$, $\mathbf{H}_{\text{SC+DMC}}$ and $\mathbf{H}_{\text{SC+DMC+Noise}}$, the channel matrices are normalised to the mean signal power, which is known from the parameter estimation:

$$\widehat{\mathbf{H}} = \frac{\mathbf{H}}{\sqrt{\frac{\sum_{m_f=0}^{M_f-1}\|\mathbf{H}_{\text{Meas}}(\Delta f\cdot m_f)\|_F^2}{M_{Tx}\cdot M_{Rx}\cdot M_f}-\alpha_0}} \tag{9}$$

where $\mathbf{H}$ is either the measured or one of the reconstructed channel matrices. Note that in the cases of **SC+DMC** and **SC+DMC+Noise**, the mean capacity of 20 channel realisations (different DMC and noise vectors) is used.

4. Results

In here the capacities of the reconstructed channels $\mathbf{H}_{\text{SC}}$, $\mathbf{H}_{\text{SC+DMC}}$, $\mathbf{H}_{\text{SC+DMC+Noise}}$ and the measured channel $\mathbf{H}_{\text{Meas}}$ of a 4×4 MIMO system are compared. Two adjacent polarimetric patch antennas at the Tx and Rx side are chosen. The capacities (eqn. (8)) are calculated for application SNRs between -10 dB and 20 dB. In Fig. 1(a) the capacities (application SNR=0dB) for all cases are plotted with respect to the snapshot index. The dashed lines divide the total measurement route in 5 segments, where the dominating propagation condition of each segment is specified. Under all conditions the $\mathbf{H}_{\text{SC}}$ case has the lowest capacity and is most constant over the entire measurement route. The capacity of the noise-free reconstructed channel ($\mathbf{H}_{\text{SC+DMC}}$) is around 20% to 50% higher than using just the specular components for the reconstruction, where the only exception is the LoS condition. Note that assuming a perfect match of our model (eqn. (1)) with the real world channel, the capacity of the channel $\mathbf{H}_{\text{SC+DMC}}$ case is the maximum available capacity that can be achieved with the used MIMO system in this environment. Since, a measured noise free channel is not available this hypothesis can only be verified by comparing the capacity of $\mathbf{H}_{\text{Meas}}$ with the capacity of the noisy reconstructed channel $\mathbf{H}_{\text{SC+DMC+Noise}}$. In Fig. 1(a) it can be observed that both of these cases (black and yellow plots) are almost matching. Under the assumption that the **SC+DMC** capacity is the realistic capacity, the relative capacity error of the other cases is defined as follows:

$$E_{\text{Cap.}} = 100\cdot\frac{(C_{\mathbf{SC+DMC}}-C)}{C_{\mathbf{SC+DMC}}}\;\;[\%] \tag{10}$$

where C is the capacity of one of the other cases. In Fig. 1(b) this relative error is plotted, where negative values correspond to an over-estimated capacity and positive values correspond to under estimation. Mainly in the NLoS regions the capacity is under-estimated using the channel $\mathbf{H}_{\text{SC}}$, where at the same position the capacity calculated from the measurement is over-estimated since the measurement noise is assumed as channel diversity. The capacity error of the $\mathbf{H}_{\text{SC}}$ and $\mathbf{H}_{\text{Meas}}$ under LoS condition is almost negligible due to the high specular power and the higher measurement SNR respectively.

In the following, the capacities are compared for application SNRs between -10 dB and 20 dB. Therefore, the mean capacity of all snapshots in each segment is calculated w.r.t. to the chosen application SNR. Under LoS condition it becomes obvious (See Fig. 2(a)), that especially for higher application SNRs the noise-free reconstructed channel ($\mathbf{H}_{\text{SC+DMC}}$) achieves a higher capacity than the noisy $\mathbf{H}_{\text{Meas}}$ itself. The cause of this is the high probability of closely spaced path around LoS that can not be resolved as SCs and consequently need to be modelled as DMC. This results in a model mismatch, which leads to inaccurate estimates of the DMC parameters. Using these estimates in the reconstruction step leads to an apparently higher capacity especially in the case of the higher application SNRs. Nevertheless, using the reconstructed channel $\mathbf{H}_{\text{SC+DMC}}$ is appropriate until 10 dB SNR. Furthermore, the overestimation for higher application SNRs is not more than 5%. Under NLoS condition (See Fig. 2(b)) even for high application SNRs the capacity of $\mathbf{H}_{\text{Meas}}$ and the noisy reconstructed channel $\mathbf{H}_{\text{SC+DMC+Noise}}$ are equivalent. Consequently, the proposed data model comprising the SCs and DMCs match the measurement

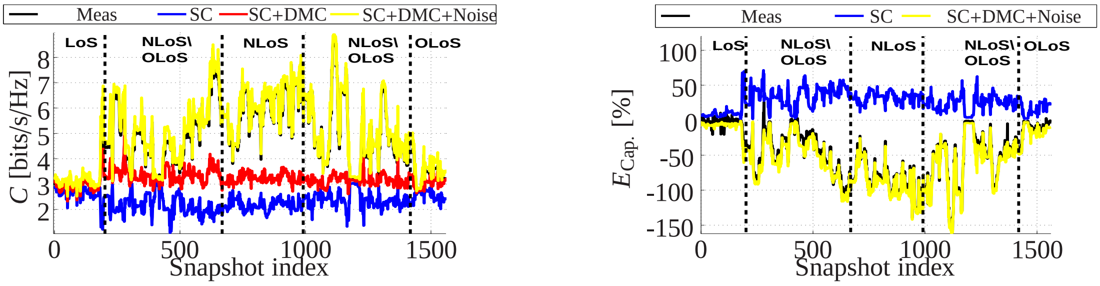

(a) (b)

Figure 1: (a) Capacities assuming a application SNR of 0 dB, (b) Relative capacity error related to the capacity of the reconstructed channel $\mathbf{H}_{\text{SC+DMC}}$

perfectly. Comparing the capacities of $\mathbf{H}_{\text{SC}}$ and $\mathbf{H}_{\text{SC+DMC}}$ it becomes obvious that the power of the specular components dominates and the influence of the DMCs increases especially for higher application SNRs.

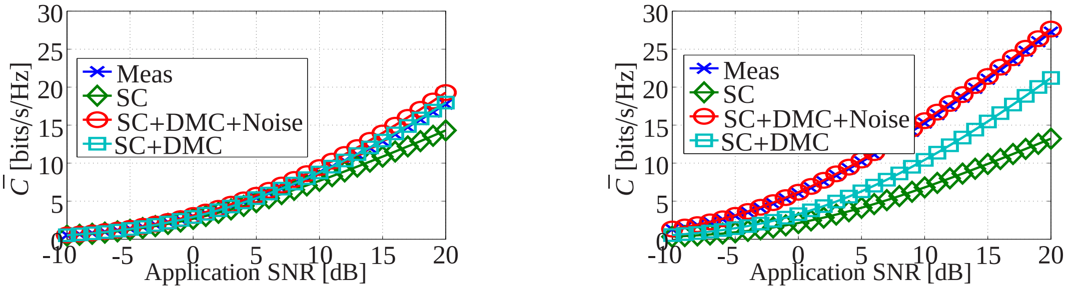

(a) LoS (b) NLoS

Figure 2: Mean capacity $\bar{C}$ under (a) LoS and (b) NLoS condition w.r.t. application SNR

5. Conclusions

In our contribution the MBPCM approach considering distributed diffuse scattering and neglecting it has been demonstrated. The results in terms of the achievable MIMO capacity of a 4×4 system clearly show, that the diffuse scattering has to be taken into account in the channel reconstruction. Furthermore, it is pinpointed that the importance of modelling the DMC is dependent on the application SNR, which is used for capacity calculation.

References

[1] M. Haardt, R.S. Thoma and A. Richter, "Multidimensional High-Resolution Parameter Estimation with Applications to Channel Sounding", *Yingbo Hua et al. (Ed.): High-Resolution and Robust Signal Processing*, Marcel Dekker, p. 253-337, 2003

[2] B.H. Fleury, M. Tschudin, R. Heddergott, et. al., "Channel Parameter Estimation in Mobile Radio Environment Using the SAGE Algorithm", *IEEE Journal on Selected Areas in Comm.*, VOL. 17, NO. 3, pp. 434-450, March 1999.

[3] R. Thoma, et. al., "Measurement-based parametric channel modeling (MBPCM)", *Proc. of the International Conf. on Electromagnetics in Advanced Applications (ICEAA03)*, Torino, Italy, Sep. 2003.

[4] R.S. Thoma, M. Landmann, A. Richter, et. al., "Multidimensional High-Resolution Channel Sounding", *in T. Kaiser et. al. (Ed.), Smart Antennas in Europe - State-of-the-Art, EURASIP Book Series on SP&C, Hindawi Publishing Corporation*, Vol. 3, 2005.

[5] J.W. Wallace and M.A. Jensen, "Validation of parametric directional MIMO channel models from wideband FDTD simulations of a simple indoor environment", *2003 IEEE AP-S International Symposium Digest, Vol. 2, pp. 535-538*, Columbus, OH, June 22-27, 2003.

[6] A. Richter, J. Salmi, V. Koivunen, "Distributed scattering in radio channels and its contribution to MIMO channel capacity", *Proc. EuCAP 2006*, Nice, France, Nov. 2006

[7] http://www.channelsounder.de

[8] M. Landmann, K. Sivasondhivat, J.-I. Takada, I. Ichirou, R. Thoma, "Polarisation Behaviour of Discrete Multipath and Diffuse Scattering in Urban Environments at 4.5GHz", *EURASIP Journal on Wireless Comm. and Networking, Special Issue on Space-Time Channel Modeling for Wireless Comm.*, accepted, Jan. 2007